12. Teoremas KAM e de Poincaré-Birkhoff

PGF 5005 - Mecânica Clássica

web.if.usp.br/controle

(Referências principais: Reichl, *The Transition to Chaos*,1992; Lichtenberg e Lieberman, *Regular and Chaotic Motion*, 1992)

IFUSP

2023

Cenário para o surgimento de Caos em Sistemas Quase Integráveis

- Teorema KAM – Superfícies toroidais invariantes sobrevivem à perturbação. Trajetórias caóticas ocupam regiões de superfícies destruidas.

- Teorema Poincaré-Birkhoff – Ilhas são criadas nas regiões com superfícies toroidais racionais.

Superfícies toroidais
Sistemas integráveis

r = 1

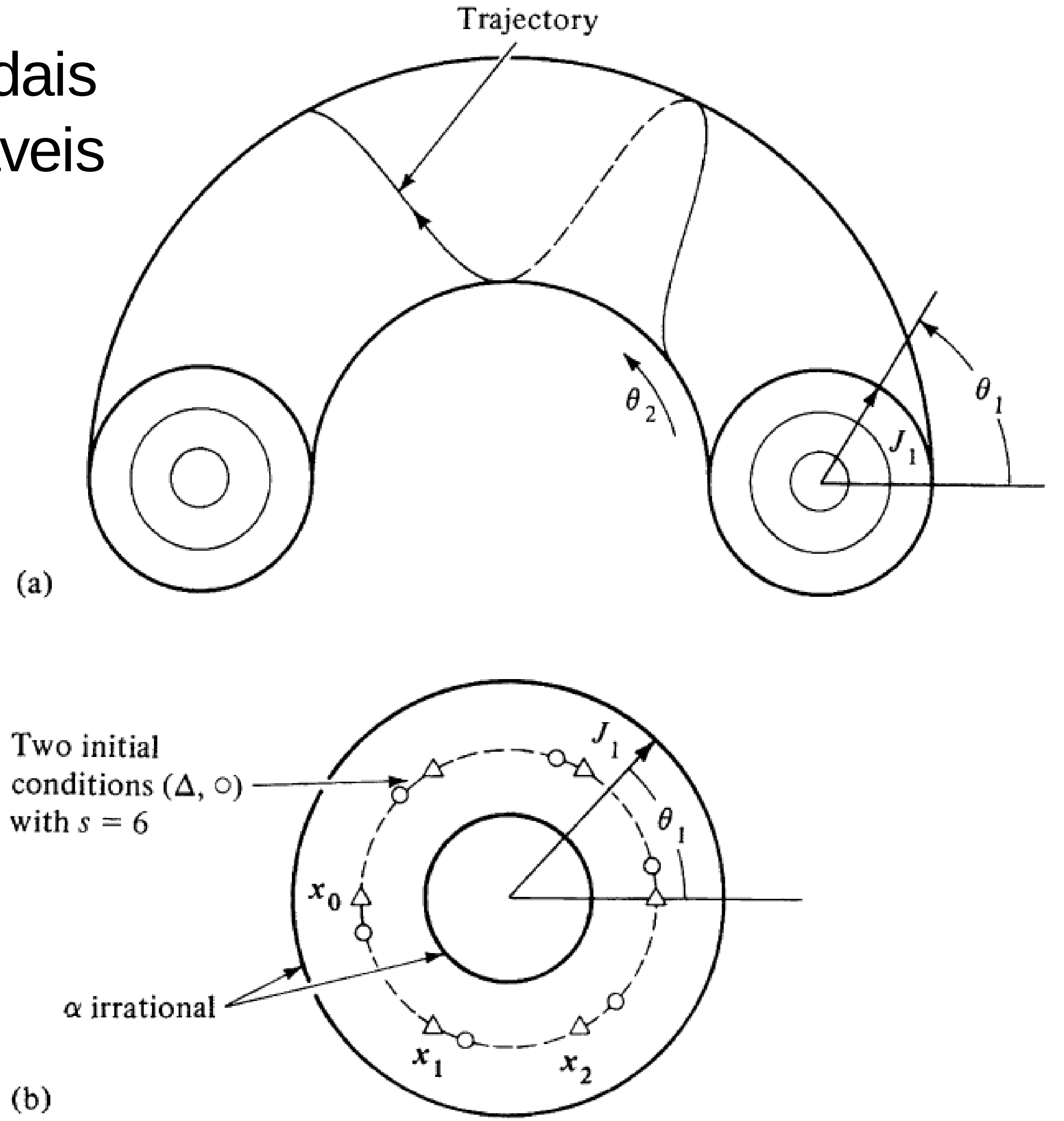

Figure 3.1. Motion of a phase space point for an integrable system with two degrees of freedom. (a) The motion lies on a torus $J_1 = \text{const.}$, $J_2 = \text{const.}$ (b) Illustrating trajectory intersections with a surface of section $\theta_2 = \text{const.}$ after a large number of such intersections.

Teorema KAM (Teorema Fundamental)

$$H(\boldsymbol{J}, \boldsymbol{\theta}) = H_0(\boldsymbol{J}) + \epsilon H_1(\boldsymbol{J}, \boldsymbol{\theta})$$

Sistema quase integrável com superfícies toroidais remanescentes

Nevertheless, it is possible to prove a theorem (the KAM theorem) that, provided certain conditions are satisfied (to be enumerated below), there exists an invariant torus $(\boldsymbol{J}, \boldsymbol{\theta})$ parametrized by ξ, satisfying the relations

$$\boldsymbol{J} = J_0 + \mathbf{v}(\boldsymbol{\xi}, \epsilon) \tag{3.2.1a}$$

and

$$\boldsymbol{\theta} = \boldsymbol{\xi} + \boldsymbol{u}(\boldsymbol{\xi}, \epsilon). \tag{3.2.1b}$$

Here $\boldsymbol{u}$ and $\mathbf{v}$ are periodic in $\boldsymbol{\xi}$ and vanish for $\epsilon = 0$, and $\dot{\boldsymbol{\xi}} = \boldsymbol{\omega}$, the unperturbed frequencies on the torus. The conditions to be satisfied are

The conditions to be satisfied are

(1) the linear independence of the frequencies

$$\sum_i m_i \omega_i(\boldsymbol{J}) \neq 0 \tag{3.2.2}$$

over some domain of $\boldsymbol{J}$ (sufficient nonlinearity), where the ω_i are the components of $\boldsymbol{\omega} = \partial H_0/\partial \boldsymbol{J}$ and the m_i are the components of the integer vector $\boldsymbol{m}$;

(2) a smoothness condition on the perturbation (sufficient number of continuous derivatives of H_1);

(3) initial conditions sufficiently far from resonance to satisfy

$$|\boldsymbol{m} \cdot \boldsymbol{\omega}| \geqslant \gamma |\boldsymbol{m}|^{-\tau} \tag{3.2.3}$$

for all $\boldsymbol{m}$, where τ is dependent on the number of degrees of freedom and the smoothness of H_1, and γ is dependent on ϵ, on the magnitude of the perturbation Hamiltonian H_1, and on the nonlinearity G of the unperturbed Hamiltonian H_0.

Since (3.2.3) cannot be met for γ too large, and γ increases with ϵ, $|H_1|$, and $1/G$, there is a condition of sufficiently small perturbation for KAM tori to exist. Conditions (1) and (2) also imply a condition of *moderate nonlinearity*. If the conditions of the theorem are met, then the circle of a twist mapping perturbs to a near-circle, as shown in Fig. 3.2a, without change of topology. This is the intersection of a KAM torus with a surface of section.

The theorem was proved by Arnold (1961, 1962, 1962b) for analytic H_1 (all derivatives existing), following a conjecture by Kolmogorov (1954), and by Moser (1962) for a sufficient number of continuous derivatives. It provides the basis for the existence of invariants in nonlinear coupled systems. The theorem is generally called the KAM theorem in recognition of their work.

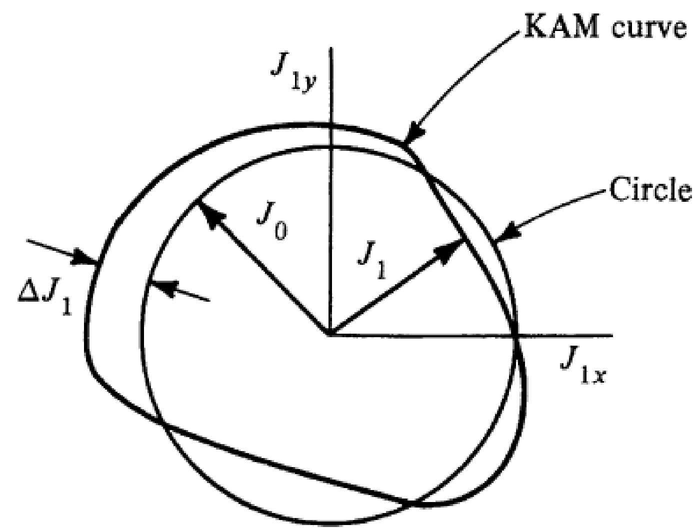
KAM curve
J_{1y}
Circle
J_0
J_1
ΔJ_1
J_{1x}

(a)

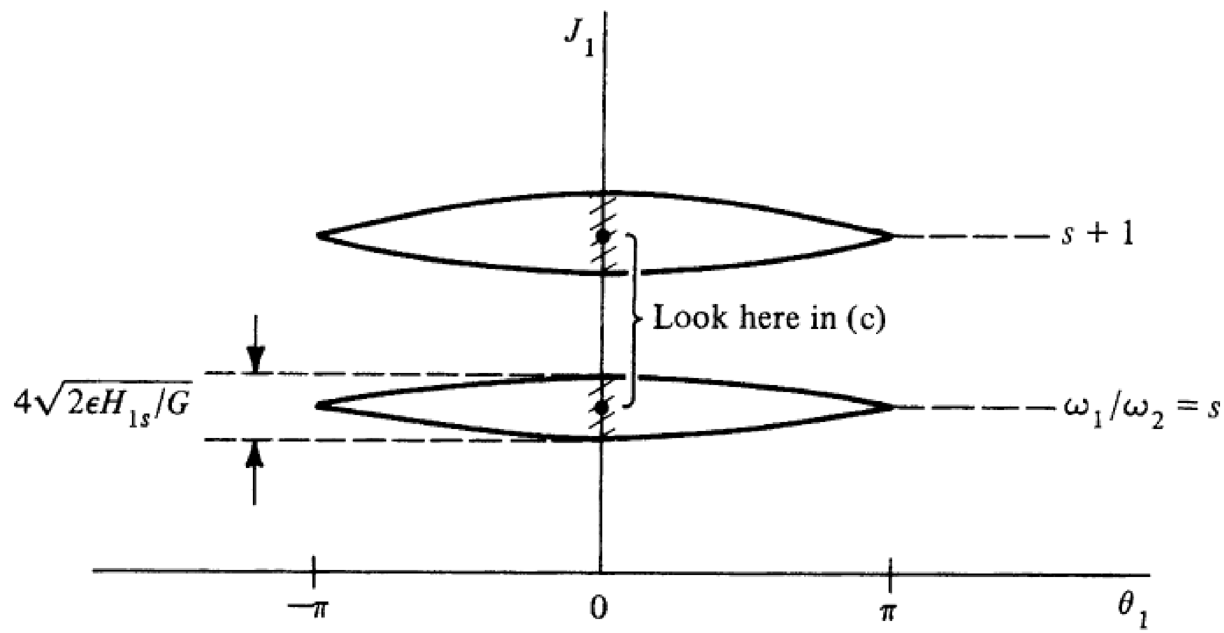
J_1
$s + 1$
Look here in (c)
$4\sqrt{2\epsilon H_{1s}/G}$
$\omega_1/\omega_2 = s$
$-\pi$
0
π
θ_1

(b)

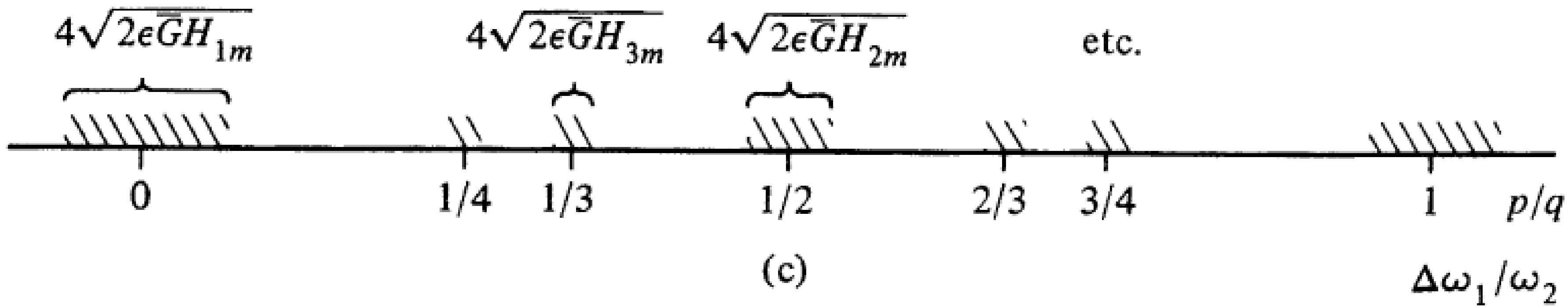

(c)

Figure 3.2. Conditions for the KAM theorem to hold. (a) Illustration of the sufficient nonlinearity condition discussed in the text; the perturbed curve lies near the unperturbed curve. (b) Illustration of the smoothness condition; the region between primary resonances is examined for secondary resonances. (c) The action region between two primary resonances converted to a frequency scale using $\Delta\omega = G\Delta J$. Secondary resonances are shown hatched. For sufficient smoothness, the secondary resonances are isolated.

We continue our examination of the perturbed twist map, given by (3.1.13). We have seen that if we examine irrational surfaces sufficiently far from the rational $\alpha = r/s$, the KAM theorem tells us that the surfaces retain their topology and are only slightly deformed from the unperturbed circles. However, on the rational surface $\alpha = r/s$, and in a neighborhood about it, the KAM theorem fails. For this region we can fall back on an earlier theorem for some clue to the structure of the mapping near rational α.

Poincaré–Birkhoff Theorem. For the unperturbed twist mapping (3.1.8), we have seen that *any* point on the circle $\alpha(J) = r/s$ is a fixed point of the mapping with period s (see Fig. 3.1b). The theorem states that for some even multiple of s, i.e., $2ks$ ($k = 1, 2, \ldots$), fixed points remain after the perturbation. The theorem is easy to prove and the proof can be outlined, using Fig. 3.3, as follows.

If we assume for definiteness that $\alpha(J)$ increases outward (strong spring), then there is a KAM curve outside the rational surface, which for s iterations of the mapping maps counterclockwise (outside arrows) $\alpha > r/s$, and one inside the rational surface, which maps clockwise (inside arrows) $\alpha < r/s$. Therefore between these two there must be a curve (solid line, not a KAM curve) whose angular coordinate θ is unchanged after s iterations of the mapping. These points are then radially mapped from the solid curve to some dashed curve (not a KAM curve), as shown in the figure. Due to the area-preserving property of the transformation, the solid and dashed curves must enclose an equal area. This is only possible if the two curves cross each other an even number of times. Each crossing when iterated s times returns to its initial position, so each of the s iterates is itself a fixed point. Thus, for an even number of crossings, there must be $2ks$ such points, which are the Poincaré–Birkhoff fixed points.

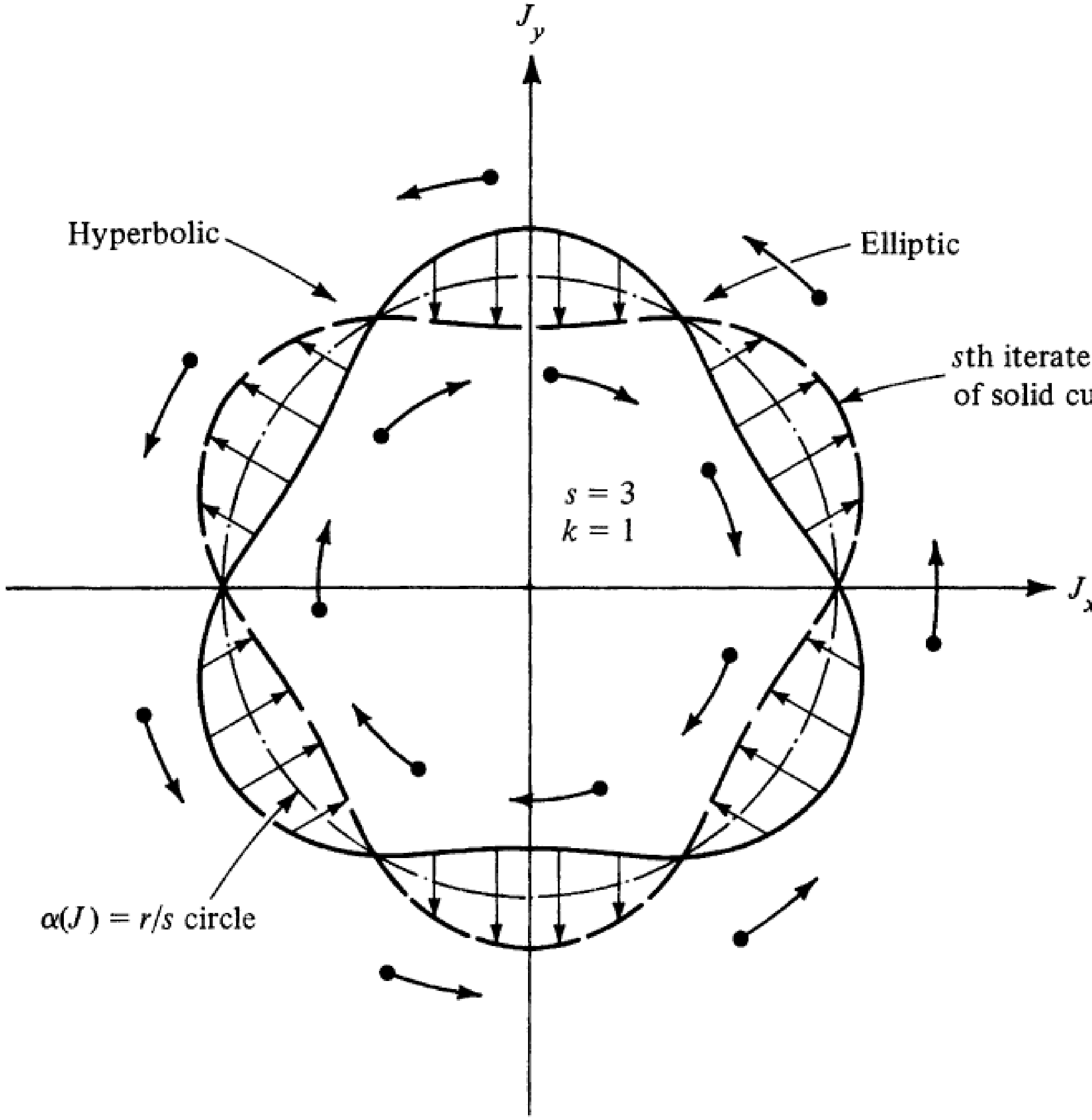

Figure 3.3. Illustrating the Poincaré–Birkhoff theorem that some fixed points are preserved in a small perturbation. The intersections of the heavy solid and dashed curves are the preserved fixed points.

The theorem makes no claim about the value of the integer k, although generally $k = 1$. If we further examine the mapping in the neighborhood of the fixed points, we notice in Fig. 3.3 that there are two distinct types of behavior. Near the fixed point labeled *elliptic*, points with $\alpha \neq r/s$, tend to connect with the $\alpha = r/s$ radial transformation, and thus to circle about the fixed point. Near the fixed point labeled *hyperbolic*, on the other hand, successive transformations take the points further from the neighborhood of the fixed point. This behavior has already been noted for the phase space motion of a simple pendulum or nonlinear spring in Section 1.3. We found

chains of alternating elliptic and hyperbolic singular points, with regular phase space trajectories encircling the elliptic fixed points and a separatrix trajectory connecting the hyperbolic points. For small perturbation amplitudes, the alternation of elliptic and hyperbolic singular points about the resonance curve is a generic property of the system.

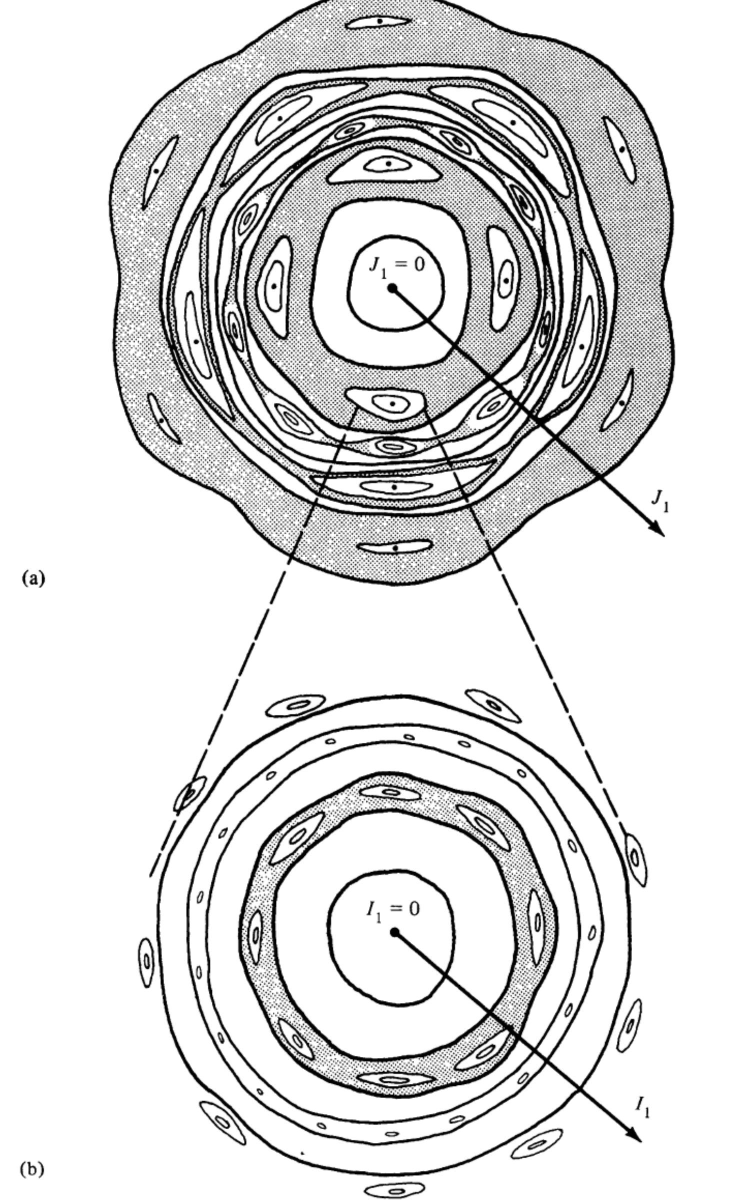

Figure 3.5. Regular and stochastic trajectories for a Hamiltonian with relatively large perturbation (a) near the primary fixed point; (b) expanded (and circularized) scale near a second-order fixed point.

Exemplo Numérico

Here we illustrate some of the phenomena previously discussed in this section with two examples, the first being the quadratic twist mapping studied by Hénon (1969):

$$\begin{pmatrix} x_1 \\ y_1 \end{pmatrix} = T\begin{pmatrix} x_0 \\ y_0 \end{pmatrix} = \begin{bmatrix} x_0 \cos\psi - (y_0 - x_0^2)\sin\psi \\ x_0 \sin\psi + (y_0 - x_0^2)\cos\psi \end{bmatrix}, \tag{3.2.40}$$

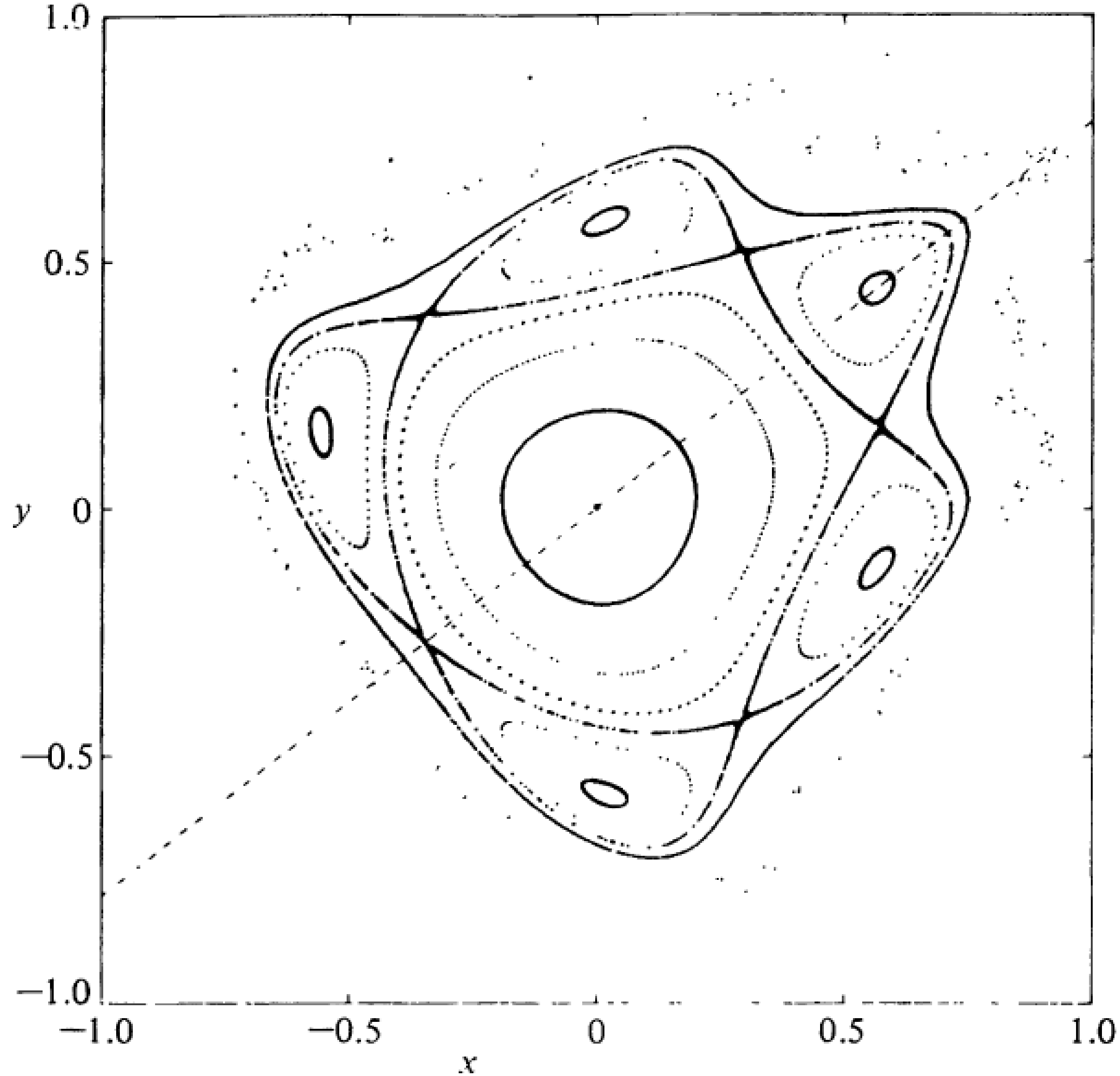

(a)

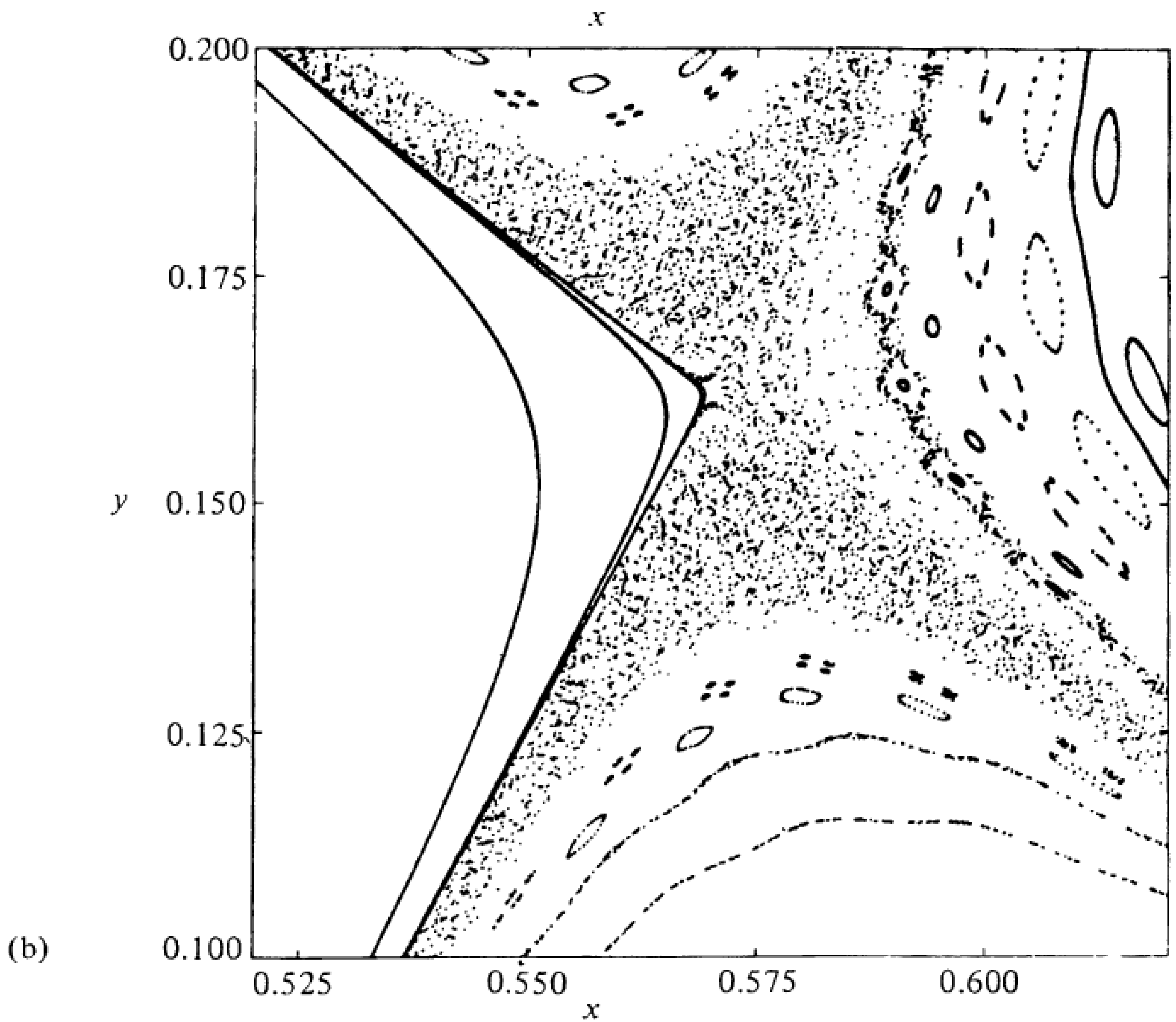

Figure 3.6. Trajectories of the Hénon mapping [Eqs. (3.2.40)] with $\alpha = 0.2114$. (a) Mapping including the origin and the first island chain; (b) expanded mapping near a separatrix of the first island chain. Each island chain, etc., is generated from a single (x_0, y_0) (after Hénon, 1969).

3.2.3 Birkhoff Fixed Point Theorem

We have seen that, for $\epsilon = 0$, the points on a given circle become dense in $\lim_{n\to\infty} T_o^n$ for irrational winding number w and are composed of discrete periodic points if w is a rational fraction. If $w = \frac{N}{M}$, the points are fixed points under the mapping T_0^M. The behavior of these fixed points under the perturbed mapping T_ϵ is extremely important and is the subject of the Birkhoff fixed point theorem [Birkhoff 1927], [Berry 1978]. Let us consider a circle, C, with winding number $w = \frac{N}{M}$ and two neighboring circles, C_+ and C_-, with irrational winding numbers $w_+ > \frac{N}{M}$ and $w_- < \frac{N}{M}$, respectively (see Fig. 3.2.2.a).

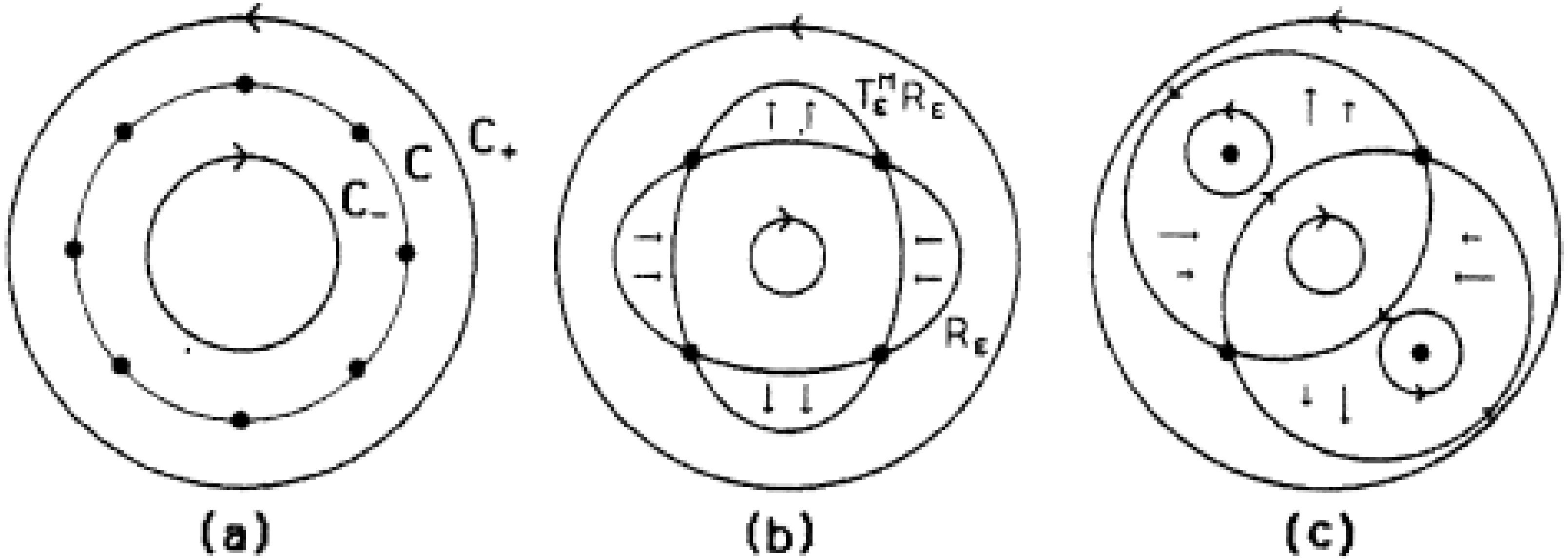

Figure 3.2.2. (a) The case $\epsilon = 0$. C is a line of orbits with period M. C_+ and C_- are orbits with irrational winding number. Under T_o^M, the periodic orbits are fixed points, while C_+ and C_- are mapped in opposite directions. (b) T_ϵ^M maps C to orbit R_ϵ and maps R_ϵ to orbit $T_\epsilon^M R_\epsilon$. By area conservation, intersections occur in an even number of places and are fixed points of T_ϵ^M. (c) The direction of flow shows that fixed points are alternating elliptic and hyperbolic.

under T_ϵ^M. Thus, all points of intersection are fixed points of T_ϵ^M. We see then that the number of intersections must be an even multiple of M, i.e., there are $2kM$ fixed points of T_ϵ^M, where k is an integer. From the direction of the flow of phase points in the neighborhood of these fixed points, we see that half must be elliptic fixed points and half must be hyperbolic fixed points (see Fig. 3.2.2.c). If we move the origin of our mapping to any elliptic point, this picture will repeat itself (see Fig. 3.2.3).

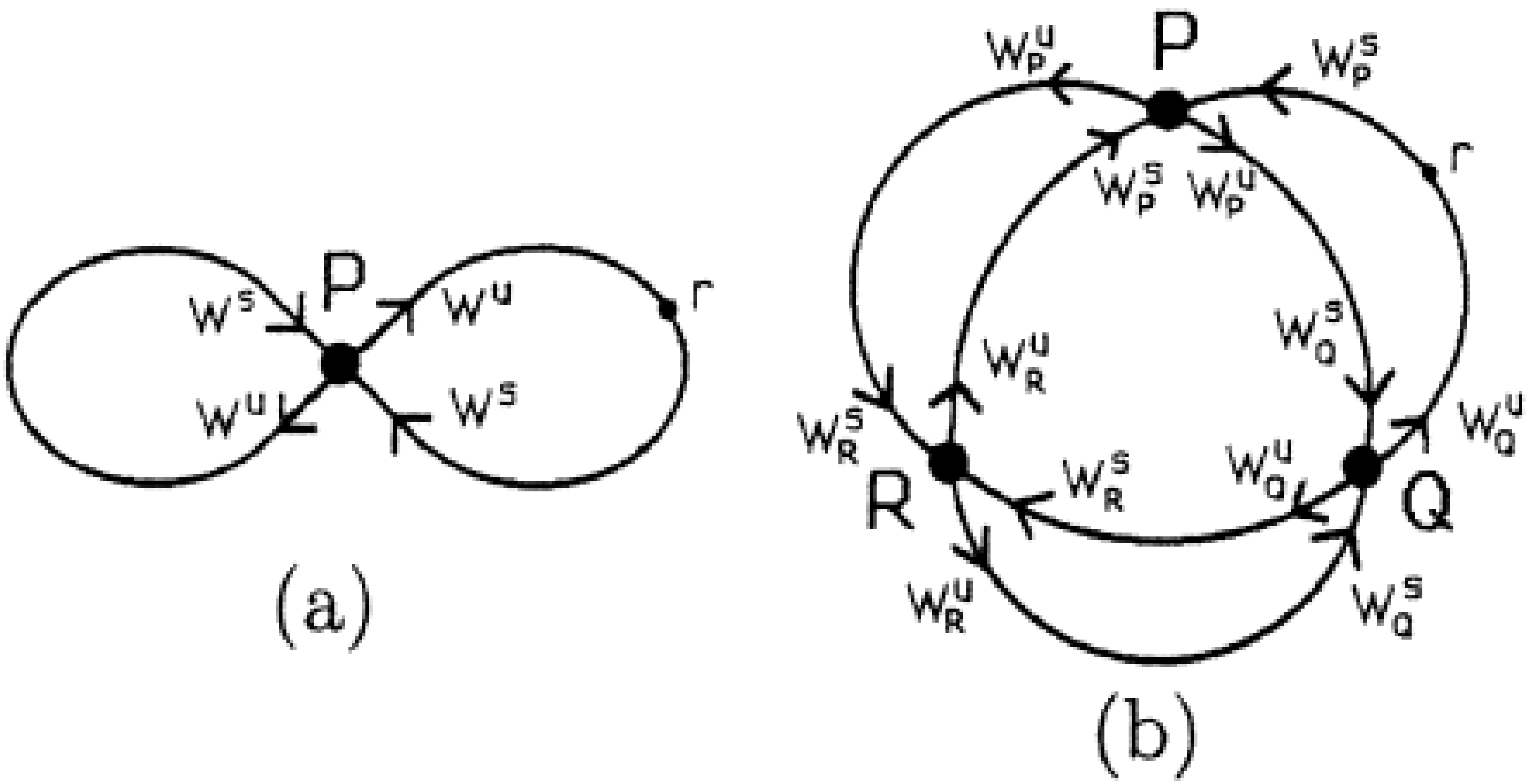

Figure 3.2.5. The stable and unstable manifolds, W^s and W^u, of hyperbolic fixed points for integrable systems join smoothly. (a) A point r on $W^{(s)}$ and $W^{(u)}$ is mapped to the same fixed point, P, by T_o and T_o^{-1}. (b) A point r on $W^{(s)}$ and $W^{(u)}$ is mapped to fixed point P by T_o and to fixed point Q by T_o^{-1}.